Radiology

Three-dimensional Dynamic Contrast-enhanced US Imaging for Early Antiangiogenic Treatment Assessment in a Mouse Colon Cancer Model[1]

Huaijun Wang, MD, PhD
Dimitre Hristov, PhD
Jiale Qin, MD[2]
Lu Tian, PhD
Jürgen K. Willmann, MD

Purpose: To evaluate feasibility and reproducibility of three-dimensional (3D) dynamic contrast material–enhanced (DCE) ultrasonographic (US) imaging by using a clinical matrix array transducer to assess early antiangiogenic treatment effects in human colon cancer xenografts in mice.

Materials and Methods: Animal studies were approved by the Institutional Administrative Panel on Laboratory Animal Care at Stanford University. Three-dimensional DCE US imaging with two techniques (bolus and destruction-replenishment) was performed in human colon cancer xenografts (n = 38) by using a clinical US system and transducer. Twenty-one mice were imaged twice to assess reproducibility. Seventeen mice were scanned before and 24 hours after either antiangiogenic (n = 9) or saline-only (n = 8) treatment. Data sets of 3D DCE US examinations were retrospectively segmented into consecutive 1-mm imaging planes to simulate two-dimensional (2D) DCE US imaging. Six perfusion parameters (peak enhancement [PE], area under the time-intensity curve [AUC], time to peak [TTP], relative blood volume [rBV], relative blood flow [rBF], and blood flow velocity) were measured on both 3D and 2D data sets. Percent area of blood vessels was quantified ex vivo with immunofluorescence. Statistical analyses were performed with the Wilcoxon rank test by calculating intraclass correlation coefficients and by using Pearson correlation analysis.

Results: Reproducibility of both 3D DCE US imaging techniques was good to excellent (intraclass correlation coefficient, 0.73–0.86). PE, AUC, rBV, and rBF significantly decreased ($P \leq .04$) in antiangiogenic versus saline-treated tumors. rBV (r = 0.74; P = .06) and rBF (r = 0.85; P = .02) correlated with ex vivo percent area of blood vessels, although the statistical significance of rBV was not reached, likely because of small sample size. Overall, 2D DCE-US overestimated and underestimated treatment effects from up to 125-fold to170-fold compared with 3D DCE US imaging. If the central tumor plane was assessed, treatment response was underestimated up to threefold or overestimated up to 57-fold on 2D versus 3D DCE US images.

Conclusion: Three-dimensional DCE US imaging with a clinical matrix array transducer is feasible and reproducible to assess tumor perfusion in human colon cancer xenografts in mice and allows for assessment of early treatment response after antiangiogenic therapy.

[1] From the Department of Radiology, Molecular Imaging Program at Stanford (H.W., J.Q., J.K.W.), Department of Radiation Oncology (D.H.), and Department of Health, Research & Policy (L.T.), Stanford University School of Medicine, 300 Pasteur Dr, Room H1307, Stanford, CA 94305-5621. Received December 9, 2014; revision requested January 19, 2015; revision received January 25; accepted February 25; final version accepted March 12. H.W. supported by the Stanford Dean Fellowship award. J.K.W. supported by the Developmental Cancer Research Award from the Stanford Cancer Center Grant and an Angel grant from the Department of Radiology. **Address correspondence to** J.K.W. (e-mail: *willmann@stanford.edu*).

[2] **Current address:** Department of Ultrasound, Women's Hospital, School of Medicine, Zhejiang University, Hangzhou, Zhejiang, China.

Colorectal cancer is the fourth most common malignancy and the second leading cause of cancer-related deaths in the United States (1). It is estimated that approximately 140 000 new cases of colorectal cancer will be diagnosed in the United States and more than 50 000 patients will die of the disease in 2014 (2). Liver metastases are present in approximately 15%–25% of patients at diagnosis and develop in about 60% of patients during the course of the disease (3).

Surgical resection is currently the standard of care for eligible patients with liver metastases from colon cancer. Chemotherapy is used preoperatively in patients with resectable and unresectable colorectal cancer liver metastases. In the former group, this confers a potential survival advantage. In the latter group, the initially unresectable colorectal cancer liver metastases can be successfully downsized in up to 40% of patients (4). The addition of a targeted agent, such as cetuximab (a monoclonal antibody that targets and inhibits the epidermal growth factor receptor) or bevacizumab (a monoclonal antibody that inhibits vascular endothelial growth factor A), can improve the efficacy of chemotherapy (5,6).

Medical imaging plays an important role in the evaluation of the response of patients with colorectal liver metastases who undergo chemotherapy. In particular, Response Evaluation Criteria in Solid Tumors is used to standardize tumor measurements in clinical care and trials. However, many targeted therapies, including bevacizumab, result in cytostatic rather than cytotoxic effects and lead to little change in tumor size despite substantial clinical benefit for the patient (7). Therefore, there is a critical need to develop noninvasive functional or molecular imaging methods to assess response to therapy and for earlier identification of responders from nonresponders. Dynamic contrast material–enhanced (DCE) computed tomographic (CT) and magnetic resonance (MR) imaging were shown to depict therapy-induced changes in tumor perfusion before there were changes in lesion size (8–11). While promising, DCE CT imaging is associated with ionizing radiation, and the use of contrast media with MR or CT imaging is limited in patients with renal insufficiency. Furthermore, there is limited access to MR imagers and the examination is relatively expensive, which renders perfusion MR imaging less practical for routine oncologic imaging.

DCE ultrasonographic (US) imaging is an attractive complementary imaging modality for evaluation of response to targeted treatment in organs that are accessible for US imaging, such as the liver. It has excellent temporal resolution (which allows for tracking of DCE), is widely available, does not expose patients to radiation, and can be performed at the bedside in patients with substantial comorbidities. Furthermore, microbubbles used as contrast agents for DCE US imaging can be safely administered in patients with renal insufficiency because they do not show any nephrotoxic effects (12,13). Two-dimensional (2D) DCE US was correlated with changes in perfusion during the first 2 weeks of treatment with the antiangiogenic agent sunitinib and subsequent overall survival in patients with metastatic renal cell carcinoma (14).

However, heterogeneity in tumor vascularity that is secondary to focal

Advances in Knowledge

- Three-dimensional (3D) dynamic contrast-enhanced (DCE) US imaging with both the bolus and destruction-replenishment acquisition techniques is feasible and reproducible (intraclass correlation coefficient, 0.73–0.86) to assess tumor perfusion in a human colon cancer xenograft model in mice.
- 3D DCE US imaging that uses both acquisition techniques allows assessment of early treatment response after antiangiogenic therapy in human colon cancer xenografts.
- The in vivo perfusion parameters relative blood volume ($r = 0.74$; $P = .06$) and relative blood flow ($r = 0.85$; $P = .02$) quantitatively correlate with the percent area of blood vessels as assessed ex vivo by immunofluorescence.
- Depending on the perfusion parameter, antiangiogenic treatment effects can be overestimated or underestimated from up to 125-fold to 170-fold on two-dimensional (2D) DCE US imaging compared with 3D DCE US imaging.

Implication for Patient Care

- The capabilities of 3D imaging may further expand the role of DCE US imaging for management of cancer, particularly to more accurately monitor molecularly targeted therapies compared with current 2D DCE US imaging.

Published online before print
10.1148/radiol.2015142824 **Content codes:** US OI

Radiology 2015; 277:424–434

Abbreviations:
au = arbitrary units
AUC = area under the time-intensity curve
DCE = dynamic contrast material enhanced
ICC = intraclass correlation coefficient
PE = peak enhancement
rBF = relative blood flow
rBV = relative blood volume
3D = three-dimensional
TTP = time to peak
2D = two-dimensional

Author contributions:
Guarantors of integrity of entire study, H.W., J.K.W.; study concepts/study design or data acquisition or data analysis/interpretation, all authors; manuscript drafting or manuscript revision for important intellectual content, all authors; approval of final version of submitted manuscript, all authors; agrees to ensure any questions related to the work are appropriately resolved, all authors; literature research, H.W., J.K.W.; clinical studies, D.H.; experimental studies, H.W., J.Q., J.K.W.; statistical analysis, H.W., L.T., J.K.W.; and manuscript editing, H.W., D.H., J.K.W.

Funding:
This research was supported by the National Institutes of Health (grants R01 CA155289 and R01DK092509).

Conflicts of interest are listed at the end of this article.

areas of necrosis, hemorrhage, or hypoxia can lead to substantial sampling errors with 2D DCE US imaging (15). Three-dimensional (3D) DCE US imaging could more accurately measure tumor perfusion for the entire target lesion, which is critically needed for longitudinal monitoring of treatment response in cancer.

The purpose of our study was to evaluate feasibility and reproducibility of 3D DCE US imaging by using a clinical matrix array transducer to assess early antiangiogenic treatment effects in human colon cancer xenografts in mice.

Materials and Methods

Mouse Tumor Model

This study was approved by the Institutional Administrative Panel on Laboratory Animal Care. Thirty-eight female nude mice (Charles River Laboratories, Hollister, Calif; 6–8 weeks old; body weight, 20–25 g) were used for the human colon cancer xenograft model. Human LS174T colon adenocarcinoma cells (ATCC, Manassas, Va) were cultured in minimum essential medium (Gibco; Life Technologies, Grand Island, NY) supplemented with 10% fetal bovine serum. At 70%–80% confluence, the tumor cells were given trypsin and 3×10^6 cells suspended in 50 μl of a basement membrane preparation (BD Matrigel; BD Biosciences, San Jose, Calif) were injected subcutaneously on the lower hind limb. Tumors were imaged 7–14 days after tumor cell injection when the tumors had reached 1–2 cm in maximum diameter (mean size, 1.6 cm), which was assessed by using an electronic caliper available on the US system.

Three-dimensional DCE US Imaging in Vivo

Imaging protocol.—All imaging experiments were performed on mice with gas anesthesia (2% isoflurane in room air, administered at 2 L/min). Mice were placed prone on a heated imaging stage. Cannulation was performed in the tail vein with a 27-gauge needle (Vevo Micromarker; VisualSonics, Toronto, Canada) attached to an injection pump (Kent Scientific, Torrington, Conn). Three-dimensional DCE US was performed with a clinical US system (iU22 Xmatrix; Philips Healthcare, Andover, Mass) equipped with a clinical matrix array transducer (X6-1, Philips Healthcare; center frequency, 3.2 MHz). The transducer was held in a fixed position by using a clamp and was coupled to the tumor with a warmed custom gel standoff for US imaging, which brought the tumor beyond the near field zone of the transducer. The distance between the transducer and the center of the tumor was set at 4 cm. The following imaging parameters were kept constant for all imaging experiments in all mice: voxel dimensions, $320 \times 110 \times 210$ μm^3; focal length, 40 mm; mechanical index, 0.05; dynamic range, 40 dB; frame rate, 1 Hz; power modulation contrast imaging mode. Commercially available contrast microbubbles (mean size, 2.6 μm; range, 2.3–2.9 μm) with a perfluorobutane gas core encapsulated by a phospholipid shell (Vevo Micromarker; Visualsonics, Toronto, Canada) were used for all DCE US experiments.

In each mouse, two well-established DCE US acquisition techniques were used to acquire 3D DCE US imaging data sets. The first method (henceforth called bolus DCE US imaging) is based on the wash-in and washout kinetics of microbubbles after bolus injection (16). First, B-mode images were acquired to outline the tumor. Then, image acquisition was switched to power modulation contrast imaging mode and 5×10^7 microbubbles (100 μL) were injected within 5 seconds at a constant injection rate by using the injection pump. Datasets were acquired continuously for 4 minutes in each mouse.

The second method (henceforth called destruction-replenishment DCE US) leveraged the ability of US imaging to manipulate the contrast agent itself (16). Microbubbles were continuously injected at a constant injection rate of 2×10^7 microbubbles per minute (40 μL/min) by using the injection pump. After 4 minutes and when steady-state enhancement was reached, five high-power destructive pulses (mechanical index, 0.77) within 5 seconds were applied to clear microbubbles from the entire tumor volume. After microbubble destruction, data were acquired continuously over a 3-minute interval.

In all mice, both DCE US acquisition techniques were applied in the same imaging session and the order was randomized. To allow clearance of microbubbles from previous injections, a waiting time of at least 30 minutes was applied between each of the two DCE US acquisition techniques (17–19). All mice tolerated the repetitive injections of contrast agents well.

Evaluation of reproducibility of 3D DCE US imaging.—In 21 tumor-bearing mice (group 1) both DCE US acquisition techniques were performed twice (Fig 1). The four different contrast agent injections were separated by a waiting time of at least 30 minutes to allow clearance of microbubbles from previous injections (17–19). All mice tolerated the four repetitive injections of contrast agents well.

Evaluation of antiangiogenic treatment effect with 3D DCE US imaging.—In 17 tumor-bearing mice, the effect of antiangiogenic treatment versus saline treatment on 3D DCE US imaging data sets was assessed. A single dose of the antiangiogenic agent bevacizumab (10 mg/kg; Avastin, Genentech, South San Francisco, Calif) was intravenously injected in nine mice (group 2), and saline only was injected in eight control mice (group 3). All mice underwent DCE US imaging by using both acquisition techniques as described above at day 0 before the treatment and at 24 hours after treatment (Fig 1). After imaging, all animals were humanely killed and tumor tissues were removed for ex vivo analysis.

Analysis of 3D DCE Datasets

Image analysis was performed by one reader (H.W., a radiologist with 3 years of experience) in random order and blinded to the treatments (antiangiogenic vs saline only) by using in-house custom software (Mevislab; Mevis Medical Solutions, Bremen, Germany) (20). A volume of interest was delineated by

Figure 1

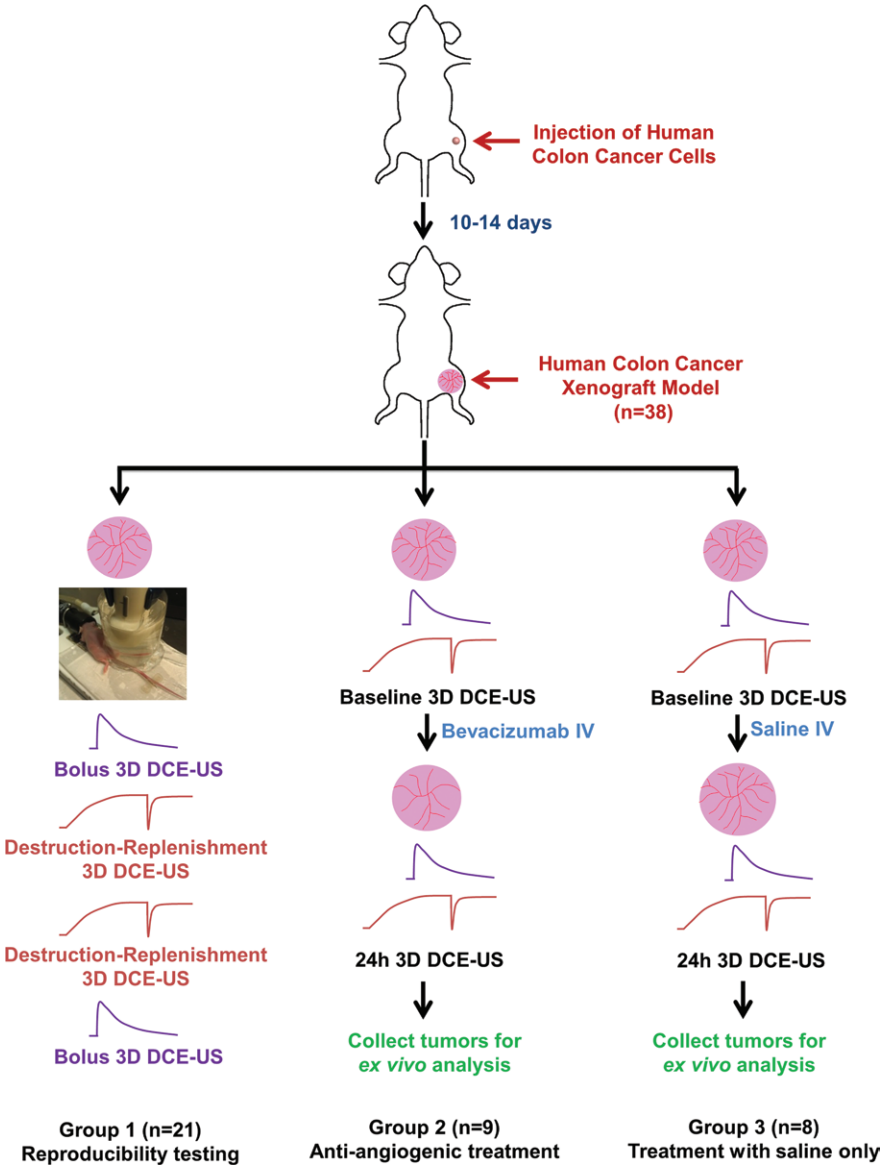

Figure 1: Overall experimental design of 3D DCE US imaging experiments. Subcutaneous human colon cancer xenografts were established in 38 nude mice and then randomized into three experimental groups. The curved lines are the time-intensity curves of 3D bolus (purple curve) or 3D destruction-replenishment (red curve) DCE US techniques.

covering the entire tumor on the 3D B-mode images viewed on axial, sagittal, and coronal imaging planes. US voxel values in power modulation contrast agent–enhanced imaging mode were linearized with a transformation function and a compression parameter provided by the equipment manufacturer. This volume of interest was subsequently used to generate time-intensity curves for the quantification of perfusion.

For the bolus DCE US imaging technique, time-intensity curves were fitted with a lognormal function model (21) and fitted curves were used to calculate the following perfusion parameters, as previously described (16,22,23): *(a)* peak enhancement (PE, related to relative blood volume, arbitrary units (au); *(b)* area under the time-intensity curve (AUC, related to relative blood volume, au); and *(c)* time to peak (TTP, seconds).

For the destruction-replenishment DCE US imaging technique, time-intensity curves were fitted with a destruction-replenishment model (24) and the fitted curves were used to calculate relative blood volume (rBV, au), relative blood flow (rBF, au), and blood flow velocity (sec^{-1}) (15,24,25). The treatment effect on 3D DCE US imaging was quantified as the ratios of PE, AUC, TTP, rBV, rBF, and blood flow velocity after and before antiangiogenic therapy in both treatment and control groups.

Comparison between 2D and 3D DCE US Acquisition Techniques

A retrospective analysis of 3D data sets into multiple consecutive 2D imaging data sets was performed to assess discrepancies in quantification of antiangiogenic treatment effects based on 3D versus 2D imaging. For this purpose, 3D data sets were segmented into multiple consecutive 1-mm-thick imaging planes (the number in each tumor was dependent on the maximum tumor diameter). All perfusion parameters, including PE, AUC, TTP, rBV, rBF, and blood flow velocity were then measured both before and after antiangiogenic treatment by drawing a region of interest that outlined the tumor boundaries in 2D. To assess the degree to which a single 1-mm imaging plane could misrepresent antiangiogenic treatment response of tumors compared with 3D imaging of the entire tumor volume, ratios of imaging signals after and before antiangiogenic treatment obtained from each 1-mm imaging plane were calculated on each 2D imaging plane and compared with the ratios of imaging signals after and before treatment obtained from 3D imaging. For central 2D imaging planes, the percent differences between 2D and 3D ratios were further calculated.

Analysis of Tumors ex Vivo

Before tumor excision, all tumors were marked on the cranial and caudal edges

(elevation direction from cranial to caudal in US imaging) and at the dorsal and left tumor surfaces by using dyes with four different colors (Davidson Marking System; Bradley Products, Bloomington, Minn). This allowed for the preservation of the spatial orientation of tumor tissues during tissue fixation and sectioning.

Tumor tissues were fixed in 4% paraformaldehyde overnight at 4°C and then cryopreserved in a 30% sucrose solution. Samples were placed in optimal cutting temperature media (Tissue-Tek; Sukura Finetek, Torrance, Calif), frozen, and then sectioned into multiple 1-mm blocks by using a cryomicrotome to allow approximate alignment with the 1-mm imaging planes reconstructed from the 3D imaging data sets. Out of each 1-mm tissue block, a representative 10-μm section from the center of the block was selected for quantification of percent area of blood vessels.

Blood vessels in tumors were made visible with standard immunofluorescence procedures. In brief, sections were incubated in phosphate-buffered saline for 10 minutes to remove remaining optimal cutting temperature media and made permeable for 10 minutes in 0.5% octoxynol-9 (Triton X-100; Sigma, St Louis, Mo) in phosphate-buffered saline. Sections were blocked in a solution that contained 3% bovine serum albumin (Sigma), 3% goat serum (Sigma), and 3% donkey serum (Sigma) for 30 minutes at room temperature before incubation with primary antibody ratio of 1:250 rat antimouse (CD31; eBioscience, San Jose, Calif). Primary antibody was made visible with a 1:250 ratio of antirat antibody (Alexafluor488 donkey antirat IgG; Invitrogen, Grand Island, NY). Samples were mounted in an aqueous mounting media (Biogenex, San Ramon, Calif), and fluorescent images were acquired by using a microscope (LSM 510 Meta Confocal Microscope; Carl Zeiss, Bernried, Germany) attached to a digital camera (Axiocam MRc; Carl Zeiss). Multiple single confocal sections (10 μm) were collected and displayed by using a magnification objective of 20×. By using software (ImageJ; National Institutes of Health, Bethesda, Md), the percentage area of blood vessels per section was quantified as the average value from at least five randomly selected fields of view (single field of view area, 0.19 mm^2) obtained from the different 1-mm tumor sections. The overall mean percentage area of blood vessels per whole tumor volume was calculated by averaging the respective values obtained from all consecutive 1-mm sections per tumor.

Statistical Analysis

To measure reproducibility of the two DCE acquisition techniques, intraclass correlation coefficients (ICCs) and 95% confidence intervals were calculated. An ICC of 0–0.20 indicated no agreement; 0.21–0.40, poor agreement; 0.41–0.60, moderate agreement; 0.61–0.80, good agreement; and greater than 0.80, excellent agreement (26). Changes in PE, AUC, TTP, rBV, rBF, and blood flow velocity at 24 hours after either antiangiogenic or saline-only treatment were compared by using a two-sample Wilcoxon rank test. To show imaging plane-to-plane variability in simulated 2D imaging, the coefficient of variation was calculated as the ratio between the standard deviation and the mean value of imaging signals from all the consecutive 1-mm planes for each tumor. The Pearson correlation coefficient (r) between in vivo 3D perfusion parameters and ex vivo percentage area of blood vessels from the same mice was calculated. The number of animals for the three different experimental groups was determined through power analysis to minimize overall use of animals according to our institution's guidelines. For experiments that assessed reproducibility, we expected an ICC of approximately 0.80 based on previous experience. Twenty-one pairs of measurements provided a 95% confidence interval of the ICC with an average length of 0.20, which is sufficiently narrow. For the two treatment groups, a minimum sample size of eight animals per group provided 80% power to detect a mean change of ±1.13 (standard deviation) with a P value of .05 before and after treatment. Similarly, a minimum sample size of eight animals per group provided 80% power to detect a difference of ±1.50 between the antiangiogenic and control saline-treated group. All statistical analyses were performed with commercially available software (IBM SPSS, version 20; IBM, Chicago, Ill). P values of .05 or less indicated significance.

Results

Reproducibility of 3D DCE US Imaging

Overall, reproducibility of both DCE US acquisition techniques was good to excellent (Table 1). The different perfusion parameters measured twice during one imaging session were not significantly different obtained with both the bolus and destruction-replenishment DCE US acquisition techniques ($P \geq .16$).

Three-dimensional DCE US Imaging for Assessment of Antiangiogenic Treatment

At baseline, tumor volumes in the control group (1740 mm^3 ± 754) were not significantly different (P = .57) from those in the antiangiogenic treatment group (1843 mm^3 ± 381). At 24 hours, tumor volumes were not significantly different (P = .94) between the two groups, with an average increase in volume of 18% ± 10% (P = .41) in the control group and by 9% ± 10% (P = .34) in the antiangiogenic treatment group.

By using both the bolus and destruction-replenishment DCE US imaging techniques, strong effects of the antiangiogenic treatment on several perfusion parameters were observed (Table 2, Fig 2). PE, AUC, rBV, and rBF significantly ($P \leq .04$) decreased at 24 hours after antiangiogenic treatment, whereas TTP and blood flow velocity did not significantly change ($P \geq .58$). In control animals treated with saline only, all perfusion parameters did not significantly change ($P \geq .38$).

Comparison of 3D versus Quasi 2D DCE US Imaging

PE, AUC, TTP, rBV, rBF, and blood flow velocity obtained from multiple 1-mm 2D imaging planes reconstructed

Table 1

Quantitative Values of Different Perfusion Parameters Obtained by Using the Bolus and Destruction-Replenishment DCE US Imaging Acquisition Techniques in Human Colon Cancer Xenografts Each Scanned Twice

Parameter	First Acquisition	Second Acquisition	ICC	*P* Value
PE (au)	$2.3 \times 10^6 \pm 2.4 \times 10^6$ (1.5×10^5, 8.0×10^6)	$2.5 \times 10^6 \pm 2.4 \times 10^6$ (1.3×10^5, 6.9×10^6)	0.83 (0.70, 0.90)	.44
AUC (au)	$1.0 \times 10^9 \pm 2.1 \times 10^9$ (3.0×10^7, 8.0×10^9)	$8.0 \times 10^8 \pm 1.3 \times 10^9$ (3.0×10^7, 5.9×10^9)	0.83 (0.63, 0.93)	.25
TTP (sec)	28.4 ± 19.7 (5.5, 89.6)	24.8 ± 14.9 (7.7, 61.0)	0.73 (0.44, 0.88)	.22
rBV (au)	$7.1 \times 10^5 \pm 4.8 \times 10^5$ (5.9×10^4, 1.6×10^6)	$7.2 \times 10^5 \pm 5.3 \times 10^5$ (5.7×10^4, 1.9×10^6)	0.86 (0.71, 0.94)	.90
rBF (au)	$1.9 \times 10^4 \pm 1.2 \times 10^4$ (3.8×10^3, 4.9×10^4)	$1.9 \times 10^4 \pm 1.4 \times 10^4$ (2.3×10^3, 5.2×10^4)	0.83 (0.66, 0.92)	.84
Blood flow velocity (sec^{-1})	0.041 ± 0.040 (0.009, 0.165)	0.034 ± 0.026 (0.004, 0.096)	0.86 (0.71, 0.93)	.16

Note.—*P* values refer to differences between first and second data acquisition. Data in parentheses are 95% confidence intervals.

Table 2

Percentage Change of Quantitative Values of Different Perfusion Parameters after Antiangiogenic and Saline-Only Treatment in Human Colon Cancer Xenografts

	Antiangiogenic Treatment ($n = 9$)		Saline-Only Treatment ($n = 8$)	
Parameter	Percentage Change	*P* Value	Percentage Change	*P* Value
PE (au)	−63 ± 23	.004	15 ± 47	.94
AUC (au)	−55 ± 28	.04	12 ± 19	.81
TTP (sec)	7 ± 42	.92	11 ± 75	.60
rBV (au)	−61 ± 26	.007	31 ± 87	.47
rBF (au)	−64 ± 23	.001	69 ± 119	.38
Blood flow velocity (sec^{-1})	−4.5 ± 52	.58	9 ± 29	.81

Note.—Values are percentage changes from baseline to 24 hours after treatment. *P* values were calculated between baseline and 24 hours after treatment.

at 1-mm increments showed substantial spatial heterogeneity of tumor perfusion, expressed as coefficients of variation, both before and after antiangiogenic treatment (Table 3, Fig 3). This heterogeneity was not significantly different ($P \geq .05$) for any perfusion parameter before or after antiangiogenic treatment (Table 3).

Dependent on the perfusion parameter calculated, antiangiogenic treatment–related perfusion changes were underestimated up to 170-fold or overestimated up to 125-fold compared with 3D imaging when 2D planes were analyzed alone (Table 4). There was no specific 2D location within the tumor volume that consistently showed discrepant results compared with 3D imaging in the different tumors analyzed.

In all tumors, treatment response was either underestimated up to threefold or overestimated up to 57-fold on central 1-mm sections versus 3D imaging (Fig 4).

Analysis of Tumors ex Vivo

After antiangiogenic treatment, percent area of blood vessels on quantitative immunofluorescence of tumors (1.8% ± 0.9%) was significantly ($P = .03$) smaller compared with saline-treated tumors (6.8% ± 4.9%). In vivo rBV ($r = 0.74$; $P = .06$) and rBF ($r = 0.85$; $P = .02$) correlated quantitatively with the percent areas of blood vessels as assessed ex vivo on quantitative immunofluorescence, although the statistical significance of rBV was not reached, which was likely because of small sample size. Other parameters correlated less with the percent area of blood vessels: PE ($r = 0.37$; $P = .42$), AUC ($r = -0.25$; $P = .59$), TTP ($r = -0.36$; $P = .43$), and blood flow velocity ($r = 0.20$; $P = .67$). Similar to in vivo perfusion imaging parameters, quantitative immunofluorescence analysis of multiple consecutive 1-mm tissue blocks showed substantial section-to-section variance of percentage area of blood vessels (coefficient of variation, 1.83 [95% confidence interval: −1.81, 5.47]) across tumors.

Discussion

This study indicates that 3D DCE US imaging with a clinical US imager and a clinical matrix array transducer is both feasible and reproducible and enables quantification of early antiangiogenic treatment response in a human colon cancer xenograft model. In particular, rBV and rBF, obtained by using the destruction-replenishment technique, correlate well with the percent vessel area measured by quantitative immunofluorescence used as reference standard. Our study also confirms substantial spatial heterogeneity of tumor perfusion and supports the use of 3D instead of 2D DCE US imaging to monitor antiangiogenic treatment response in cancer.

DCE US imaging is increasingly used in the clinic to assess treatment response and predict treatment outcomes in cancer patients (15,27–29). In 42 patients with advanced hepatocellular carcinoma treated with bevacizumab, 2D DCE US imaging correlated well with tumor response and progression-free survival (30). Furthermore, in 40 patients with metastatic renal cell carcinoma who underwent treatment

Figure 2

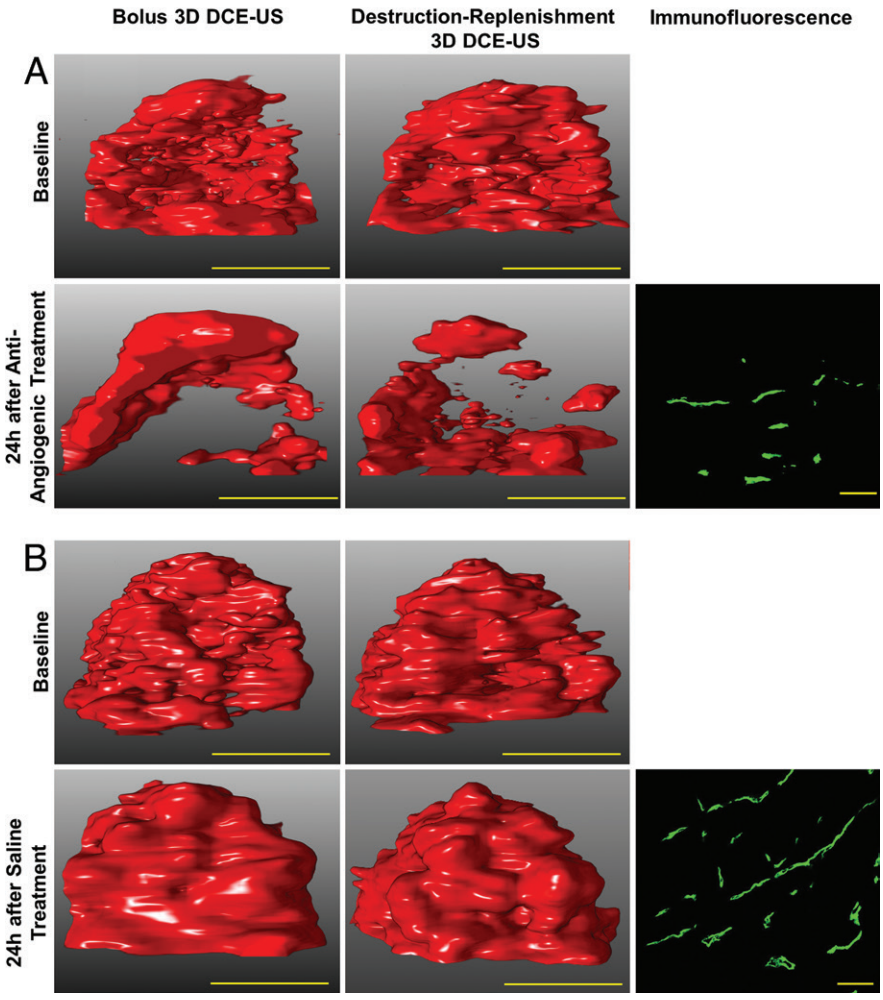

Figure 2: Three-dimensional DCE US imaging shows antiangiogenic treatment effect in two representative human colon cancer xenografts by using bolus and destruction-replenishment DCE US imaging. *A*, After a single dose of bevacizumab, imaging signal (demonstrated on volume rendered displays at peak enhancement [left] and complete replenishment [right] at identical rendering settings) substantially decreased 24 hours after antiangiogenic treatment compared with baseline images by using both DCE US imaging techniques. *B*, In tumors treated with saline only, the imaging signal did not substantially change before and after saline treatment; yellow scale bar on US images is equivalent to 10 mm. Photomicrographs of CD31-stained tissue sections show decreased percent area of blood vessels in, *A*, antiangiogenic-treated compared with, *B*, saline-treated tumor (yellow scale bar on immunofluorescence images is equivalent to 100 μm).

Table 3

Summary of the Average Coefficients of Variations Obtained from Multiple Consecutive 1-mm 2D Imaging Planes for the Different Perfusion Parameters before and after Antiangiogenic Treatment in Human Colon Cancer Xenografts

Parameter	Before Treatment	After Antiangiogenic Treatment	*P* Value
PE	0.62 (0.38, 0.86)	0.53 (0.41, 0.66)	.67
AUC	2.18 (1.13, 3.22)	2.86 (1.90, 3.90)	.27
TTP	0.72 (0.31, 1.13)	1.27 (0.73, 1.81)	.05
rBV	0.51 (0.34, 0.67)	0.68 (0.46, 0.90)	.12
rBF	1.00 (0.22, 1.77)	1.05 (0.25, 1.62)	.13
Blood flow velocity	1.17 (0.21, 2.12)	0.90 (0.16, 1.64)	.58

Note.—Other than *P* values, data are coefficients of variation; data in parentheses are 95% confidence interval range.

with sunitinib, the ratio between 2D DCE US examinations at baseline and at day 15 significantly correlated with tumor response in five of the seven quantified DCE US imaging parameters (14). However, in another study with 17 patients with metastatic renal cell carcinoma who underwent treatment with sunitinib, changes in 2D DCE US imaging parameters over 2 weeks did not correlate with progression-free survival and could not be used to predict long-term assessment of best response by using Response Evaluation Criteria in Solid Tumors (15). Substantial heterogeneity of tumor vascularity was observed in that study, which resulted in a high plane-to-plane variability with a coefficient of variation up to 41%, which could be a possible explanation for the lack of predictive value of 2D DCE US imaging in that study (15). This observation was further corroborated by recent preclinical studies. In 14 subcutaneous breast cancer tumors in mice it was shown that millimeter-sized deviations in transducer position can have profound effects on 2D US blood flow estimations, with errors that range from 6.4% to 40.3% depending on the degree of misalignment (22). In another study, 2D DCE US parametric perfusion mapping was shown to be highly dependent on the chosen imaging plane,

Figure 3

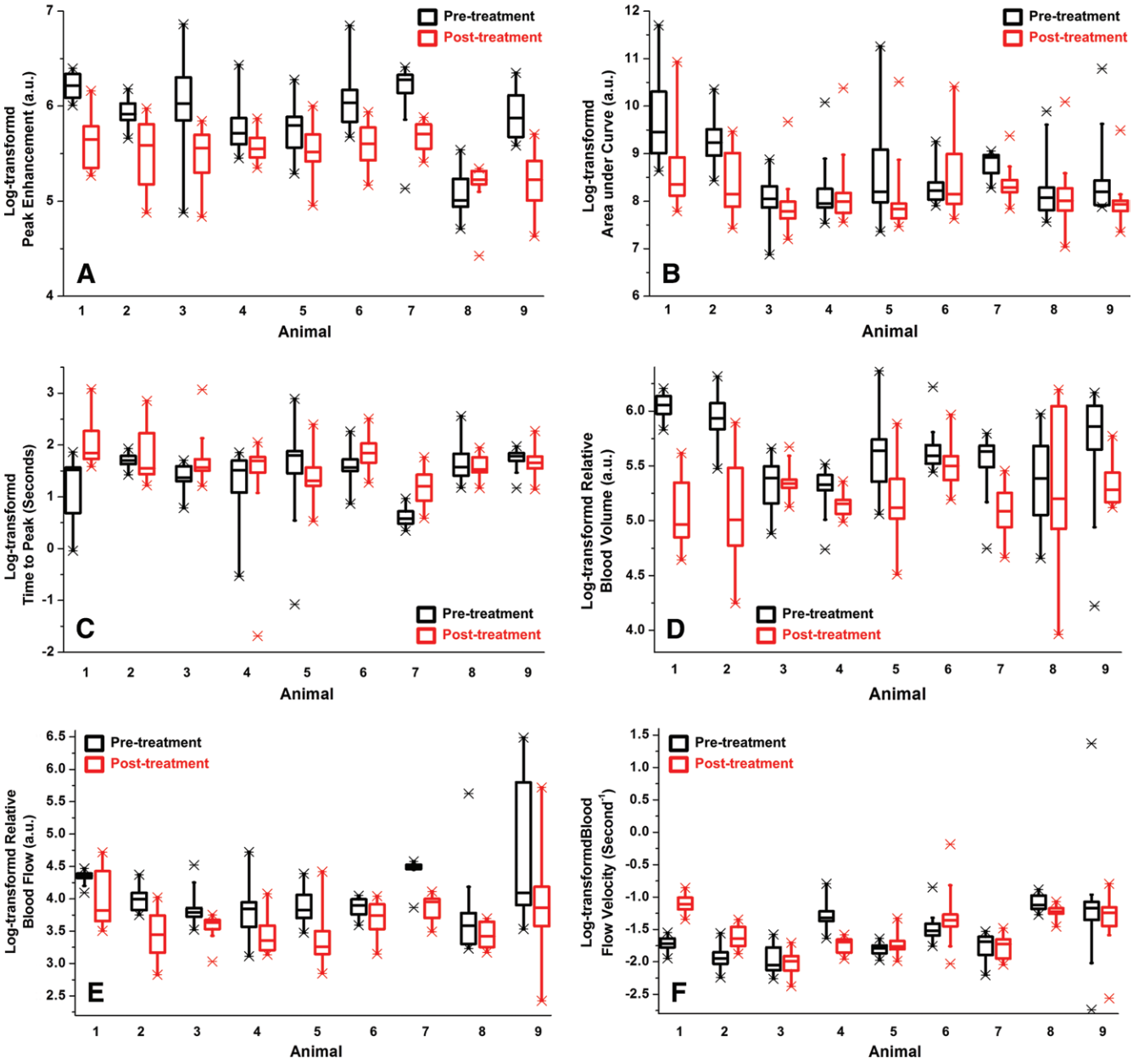

Figure 3: Box-and-whisker plots show spatial heterogeneity of tumor perfusion for all nine human colon cancer xenografts made visible with DCE US imaging before (black box plots) and 24 hours after (red box plots) antiangiogenic therapy. Three-dimensional data sets were retrospectively segmented into consecutive 1-mm data sets and logarithmically transformed perfusion parameters, including, *A*, PE, *B*, AUC, *C*, TTP, *D*, rBV, *E*, rBF, and, *F*, blood flow velocity, were plotted for each tumor separately. Each box in the plot represents the 25th and 75th quartiles, the line inside each box identifies the median, and the whiskers indicate the 5th and 95th percentile of perfusion parameter measurements. Outliers are represented by ∗. Note that there is substantial heterogeneity for all six parameters shown by the size of the boxes and the ranges of the values.

with an absolute variance of perfusion up to 22% in healthy rat kidneys (31). These results illustrate the dependence of 2D DCE US imaging on operator accuracy because the operator has to find the exact same 2D plane to accurately monitor longitudinal perfusion changes, which is not possible in clinical practice (32). They also highlight that 3D DCE US imaging techniques are needed to make DCE US imaging a more robust and clinically applicable technique (15).

Several 3D DCE US imaging approaches were recently introduced in preclinical studies. By using a linear motion

Table 4

Summary of the Average Maximum Fold Underestimation and Overestimation of Antiangiogenic Treatment Effects in Human Colon Cancer Xenografts Based on the Analysis of Consecutive 2D Data Sets Compared with 3D Data Sets

Parameter	Underestimation (fold)	Overestimation (fold)
PE (au)	7	27
AUC (au)	168	50
TTP (sec)	170	121
rBV (au)	40	78
rBF (au)	11	125
Blood flow velocity (sec^{-1})	53	83

stage to mechanically move a clinical 2D US imaging transducer (15 L8; Siemens Medical Solutions, Mountain View, Calif) at predefined step sizes, parametric maps of refill times within 10 seconds of a destructive pulse were acquired in healthy rat kidneys (31). While the sum of consecutive 2D sections provided a volumetric map of tissue perfusion, clinical applicability of this approach is limited and acquisition times are relatively long (approximately 5 minutes for a rat kidney). A more automatic approach, in which a clinical transducer (4DL14–5/38; Ultrasonix Medical Corporation, Richmond, Canada) was mechanically swept within the transducer sheath, was applied to obtain perfusion maps by using the bolus technique in a subcutaneous breast cancer model in mice (22). A similar technique was used with a probe (4D10L; GE Healthcare, Milwaukee, Wis) to make visible the vasculature at the lower pole of canine kidneys (33).

In our study, we explored the feasibility and reproducibility of quantitative 3D DCE US imaging in a human colon cancer xenograft by using a clinically available matrix array transducer (X6-1; Philips Healthcare). This transducer contains 9212 elements with an integrated microbeam former and supports volumetric DCE US imaging by electronically steering the ultrasound beam over the tumor volume. Because spacing in the y-axis is smaller with this approach than with mechanical sweeping, the transducer allows imaging at high spatial resolution and nearly constant voxel resolution in the whole imaging volume. By using both bolus and destruction-replenishment techniques, reproducibility of 3D DCE US imaging with the clinical matrix array transducer was found to be good to excellent for all perfusion parameters assessed.

We then tested whether 3D DCE US imaging allowed for early treatment response after antiangiogenic therapy in a human colon cancer model to be made visible by using both the bolus and destruction-replenishment techniques. Bolus DCE US imaging makes visible the temporal behavior of the contrast agent–induced signal after intravenous bolus injection of the contrast agent similar to DCE CT and DCE MR imaging (34,35). However, the destruction-replenishment DCE US imaging technique with constant infusion of contrast microbubbles to reach steady state does not have a CT or MR imaging analog and leverages the unique ability of US imaging to destroy the contrast agent microbubbles in the field of view. The rate of replenishment of microbubbles into the field of view after destruction is then captured and modeled by using standard indicator-dilution theory. Current models take advantage of the precise knowledge of the input function this method provides and the effect of the fractal geometry of the vasculature on the distribution of replenishment transit times (36). We found that four of six tested perfusion parameters, including PE, AUC, rBV, and rBF, significantly decreased 24 hours after a single dose of bevacizumab, while those parameters did not significantly change in saline-treated animals. Antiangiogenic treatment response was further confirmed ex vivo by estimating the percent area of blood vessels within each treated and untreated tumor by using quantitative immunofluorescence as a reference standard, and rBF correlated well with the percent area of blood vessels in our study.

Finally, we retrospectively assessed how the use of 2D instead of 3D DCE US imaging would result in different percentage of signal changes after antiangiogenic treatment. We found that, depending on the spatial location of 2D DCE US imaging within a tumor, treatment responses would substantially vary compared with 3D DCE US imaging. Depending on the perfusion parameter, those differences varied between sevenfold and 170-fold, and thus treatment responses can be both overestimated and underestimated compared with 3D DCE US imaging. For the central plane, which is usually chosen to assess treatment response in both preclinical (37) and clinical 2D DCE US examinations (15), treatment response was underestimated up to threefold and overestimated up to 57-fold.

Several limitations of our study need to be addressed. First, the number of animals in the different treatment groups was relatively small. However, strong differences between antiangiogenic and saline-only treated mice were measured. However, more confirmatory experiments are needed in additional tumor models and cancer types to further support our conclusions. Second, for this proof-of-principle study, we focused on the assessment of early antiangiogenic effects on 3D DCE US imaging signal 24 hours after treatment initiation and not over longer time intervals. Future studies are warranted in patients to assess whether early 3D perfusion changes quantified by 3D DCE US imaging are predictive of treatment response in patients with liver metastases from colorectal cancer. Another limitation is that relatively large amounts of fluid were injected, which could have influenced our results. Finally, the intra-animal comparison between 2D and 3D DCE US imaging was performed by retrospectively extracting quasi 2D data sets from the volumetric US data sets and not by prospectively imaging tumors by using both 2D and 3D DCE US imaging in the same animals. This approach was chosen for practical reasons because prospective imaging of tumors in multiple 1-mm increments would have resulted in injection of a large cumulative volume of contrast agent that is not tolerable for mice.

Our results suggest that 3D DCE US imaging with a clinical US system and matrix array transducer is

Figure 4

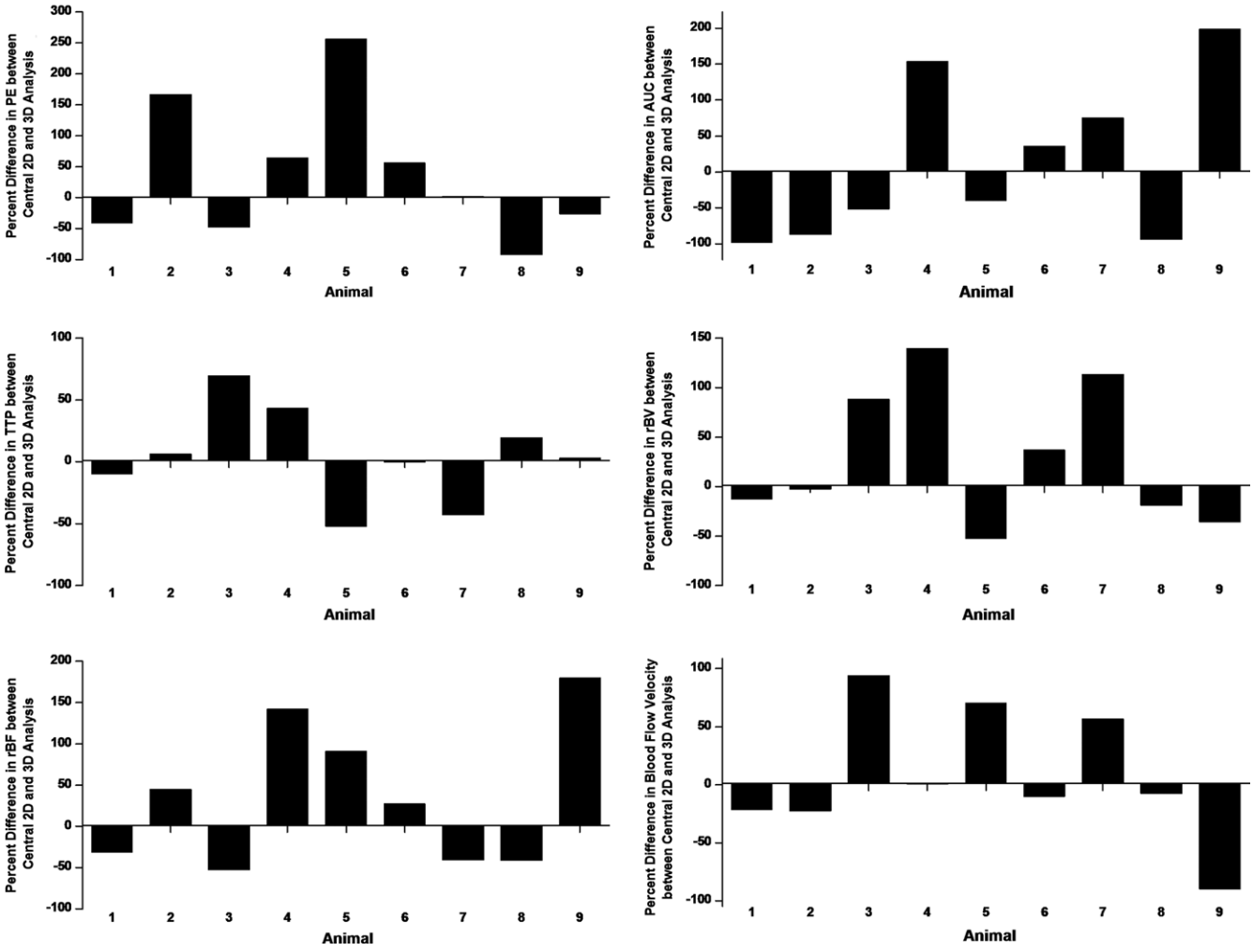

Figure 4: Bar charts plotted for all six perfusion parameters show percent differences in antiangiogenic treatment effects based on data analysis of the central 1-mm plane versus analysis of the volumetric data set for each of the nine tumors treated with antiangiogenic therapy. Ratios of each perfusion parameter after and before antiangiogenic treatment obtained from the central 1-mm plane were compared with the ratios of the perfusion parameter after and before treatment obtained from 3D imaging, and percent differences were plotted. Note that treatment response can be either over-estimated or under-estimated when analyzing the central 2D plane only compared with volumetric data set.

technically feasible and reproducible to assess tumor perfusion with both the bolus and destruction-replenishment technique. Furthermore, 3D DCE US imaging enables noninvasive quantification of antiangiogenic treatment effects as early as 24 hours after treatment initiation, which suggests that early antiangiogenic treatment effects can be assessed by 3D DCE US imaging before morphologic and anatomic changes of the tumor become visible.

Acknowledgements: We thank Vijay Shamdasani, PhD (Philips Healthcare, Bothell, Wash), for providing the clinical US system and transducer.

Disclosures of Conflicts of Interest: H.W. disclosed no relevant relationships. **D.H.** disclosed no relevant relationships. **J.Q.** disclosed no relevant relationships. **L.T.** disclosed no relevant relationships. **J.K.W.** Activities related to the present article: disclosed no relevant relationships. Activities not related to the present article: author received money for consultancy form Bracco and Triple Ring; author has grants from Siemens, GE Healthcare, and Philips. Other relationships: disclosed no relevant relationships.

References

1. Siegel R, Ma J, Zou Z, Jemal A. Cancer statistics, 2014. CA Cancer J Clin 2014;64(1):9–29.
2. American Cancer Society. Cancer Facts & Figures 2014. Atlanta, Ga: American Cancer Society, 2014.
3. Lee JJ, Chu E. Sequencing of antiangiogenic agents in the treatment of metastatic colorectal cancer. Clin Colorectal Cancer 2014; 13(3):135–144.
4. Alberts SR, Horvath WL, Sternfeld WC, et al. Oxaliplatin, fluorouracil, and leucovorin for patients with unresectable liver-only metastases from colorectal cancer: a North

Central Cancer Treatment Group phase II study. J Clin Oncol 2005;23(36):9243–9249.

5. Van Cutsem E, Köhne CH, Hitre E, et al. Cetuximab and chemotherapy as initial treatment for metastatic colorectal cancer. N Engl J Med 2009;360(14):1408–1417.

6. Bennouna J, Sastre J, Arnold D, et al. Continuation of bevacizumab after first progression in metastatic colorectal cancer (ML18147): a randomised phase 3 trial. Lancet Oncol 2013;14(1):29–37.

7. Chung WS, Park MS, Shin SJ, et al. Response evaluation in patients with colorectal liver metastases: RECIST version 1.1 versus modified CT criteria. AJR Am J Roentgenol 2012;199(4):809–815.

8. Jiang T, Kambadakone A, Kulkarni NM, Zhu AX, Sahani DV. Monitoring response to antiangiogenic treatment and predicting outcomes in advanced hepatocellular carcinoma using image biomarkers, CT perfusion, tumor density, and tumor size (RECIST). Invest Radiol 2012;47(1):11–17.

9. Anzidei M, Napoli A, Zaccagna F, et al. Liver metastases from colorectal cancer treated with conventional and antiangiogenetic chemotherapy: evaluation with liver computed tomography perfusion and magnetic resonance diffusion-weighted imaging. J Comput Assist Tomogr 2011;35(6):690–696.

10. Meier R, Braren R, Kosanke Y, et al. Multimodality multiparametric imaging of early tumor response to a novel antiangiogenic therapy based on anticalins. PLoS ONE 2014; 9(5):e94972.

11. Brufau BP, Cerqueda CS, Villalba LB, Izquierdo RS, González BM, Molina CN. Metastatic renal cell carcinoma: radiologic findings and assessment of response to targeted antiangiogenic therapy by using multidetector CT. RadioGraphics 2013;33(6):1691–1716.

12. Jakobsen JA, Oyen R, Thomsen HS, Morcos SK; Members of Contrast Media Safety Committee of European Society of Urogenital Radiology (ESUR). Safety of ultrasound contrast agents. Eur Radiol 2005;15(5):941–945.

13. Coleman JL, Navid F, Furman WL, McCarville MB. Safety of ultrasound contrast agents in the pediatric oncologic population: a single-institution experience. AJR Am J Roentgenol 2014;202(5):966–970.

14. Lassau N, Koscielny S, Albiges L, et al. Metastatic renal cell carcinoma treated with sunitinib: early evaluation of treatment response using dynamic contrast-enhanced ultrasonography. Clin Cancer Res 2010;16(4):1216–1225.

15. Williams R, Hudson JM, Lloyd BA, et al. Dynamic microbubble contrast-enhanced US to measure tumor response to targeted therapy: a proposed clinical protocol with results from renal cell carcinoma patients receiving antiangiogenic therapy. Radiology 2011;260(2):581–590.

16. Greis C. Quantitative evaluation of microvascular blood flow by contrast-enhanced ultrasound (CEUS). Clin Hemorheol Microcirc 2011;49(1-4):137–149.

17. Pysz MA, Foygel K, Panje CM, Needles A, Tian L, Willmann JK. Assessment and monitoring tumor vascularity with contrast-enhanced ultrasound maximum intensity persistence imaging. Invest Radiol 2011;46(3): 187–195.

18. Willmann JK, Cheng Z, Davis C, et al. Targeted microbubbles for imaging tumor angiogenesis: assessment of whole-body biodistribution with dynamic micro-PET in mice. Radiology 2008;249(1):212–219.

19. Palmowski M, Morgenstern B, Hauff P, et al. Pharmacodynamics of streptavidin-coated cyanoacrylate microbubbles designed for molecular ultrasound imaging. Invest Radiol 2008;43(3):162–169.

20. Heckel F, Schwier M, Peitgen HO. Object-oriented application development with MeVisLab and Python. Lect Notes Inform (Informatik 2009: Im Focus das Leben) 2009;154:1338–1351.

21. Strouthos C, Lampaskis M, Sboros V, McNeilly A, Averkiou M. Indicator dilution models for the quantification of microvascular blood flow with bolus administration of ultrasound contrast agents. IEEE Trans Ultrason Ferroelectr Freq Control 2010;57(6):1296–1310.

22. Hoyt K, Sorace A, Saini R. Quantitative mapping of tumor vascularity using volumetric contrast-enhanced ultrasound. Invest Radiol 2012;47(3):167–174.

23. Quaia E. Assessment of tissue perfusion by contrast-enhanced ultrasound. Eur Radiol 2011;21(3):604–615.

24. Wei K, Jayaweera AR, Firoozan S, Linka A, Skyba DM, Kaul S. Quantification of myocardial blood flow with ultrasound-induced destruction of microbubbles administered as a constant venous infusion. Circulation 1998; 97(5):473–483.

25. Wang JW, Zheng W, Chen Y, et al. Quantitative assessment of tumor blood flow changes in a murine breast cancer model after adriamycin chemotherapy using contrast-enhanced destruction-replenishment sonography. J Ultrasound Med 2013;32(4):683–690.

26. Faria JR, Aarão AR, Jimenez LM, Silva OH, Avelleira JC. Inter-rater concordance study of the PASI (Psoriasis Area and Severity Index). An Bras Dermatol 2010;85(5):625–629.

27. Zocco MA, Garcovich M, Lupascu A, et al. Early prediction of response to sorafenib in patients with advanced hepatocellular carcinoma: the role of dynamic contrast enhanced ultrasound. J Hepatol 2013;59(5):1014–1021.

28. Lamuraglia M, Bridal SL, Santin M, et al. Clinical relevance of contrast-enhanced ultrasound in monitoring anti-angiogenic therapy of cancer: current status and perspectives. Crit Rev Oncol Hematol 2010;73(3):202–212.

29. Zhou JH, Zheng W, Cao LH, et al. Contrast-enhanced ultrasonic parametric perfusion imaging in the evaluation of antiangiogenic tumor treatment. Eur J Radiol 2012; 81(6):1360–1365.

30. Lassau N, Koscielny S, Chami L, et al. Advanced hepatocellular carcinoma: early evaluation of response to bevacizumab therapy at dynamic contrast-enhanced US with quantification—preliminary results. Radiology 2011;258(1):291–300.

31. Feingold S, Gessner R, Guracar IM, Dayton PA. Quantitative volumetric perfusion mapping of the microvasculature using contrast ultrasound. Invest Radiol 2010;45(10):669–674.

32. Meijerink MR, van Waesberghe JH, van Schaik C, et al. Perfusion CT and US of colorectal cancer liver metastases: a correlative study of two dynamic imaging modalities. Ultrasound Med Biol 2010;36(10):1626–1636.

33. Eisenbrey JR, Sridharan A, Machado P, et al. Three-dimensional subharmonic ultrasound imaging in vitro and in vivo. Acad Radiol 2012;19(6):732–739.

34. Dietrich CF, Averkiou MA, Correas JM, Lassau N, Leen E, Piscaglia F. An EFSUMB introduction into Dynamic Contrast-Enhanced Ultrasound (DCE-US) for quantification of tumour perfusion. Ultraschall Med 2012; 33(4):344–351.

35. Hudson JM, Karshafian R, Burns PN. Quantification of flow using ultrasound and microbubbles: a disruption replenishment model based on physical principles. Ultrasound Med Biol 2009;35(12):2007–2020.

36. Hudson JM, Williams R, Karshafian R, et al. Quantifying vascular heterogeneity using microbubble disruption-replenishment kinetics in patients with renal cell cancer. Invest Radiol 2014;49(2):116–123.

37. Pitre-Champagnat S, Leguerney I, Bosq J, et al. Dynamic contrast-enhanced ultrasound parametric maps to evaluate intratumoral vascularization. Invest Radiol 2015;50(4): 212–217.